Journal of Electronic Materials, Vol. 21, No. 8, 1992

ArF Excimer Laser-Enhanced Photochemical Vapor Deposition of Epitaxial Si from Si_2H_6: A Simple Growth Kinetic Model

B. FOWLER, S. LIAN, S. KRISHNAN, L. JUNG, C. LI, D. SAMARA, I. MANNA, and S. BANERJEE

Microelectronics Research Center, University of Texas, Austin, TX 78712

Photolysis of Si_2H_6 using 193 nm radiation from an ArF excimer laser has been used to deposit homoepitaxial Si films in the temperature range of 250 to 350° C. Photolytic decomposition of Si_2H_6 generates growth precursors which adsorb on to a hydrogenated Si surface. A growth kinetic model is proposed based on single-photon 193 nm absorption by Si_2H_6, and chemical reaction of the photofragments as they diffuse to the substrate surface. With the laser beam positioned parallel to the Si substrate, the deposition yield of solid Si from photo-excited Si_2H_6 is estimated to be 0.20 ± 0.04. Growth rates vary linearly with laser intensity and Si_2H_6 partial pressure over a range of 1–15 mJ/cm^2 · pulse and 5–40 mTorr, respectively, and epitaxial films are deposited when laser intensity and Si_2H_6 partial pressure conditions are such that the initial photofragment concentration is less than $\sim 10^{13}$ cm^{-3}.

Key words: Si, Photo-CVD, growth kinetic model

1. INTRODUCTION

Low temperature silicon epitaxy can be achieved using the monochromatic 193 nm emission from an ArF excimer laser as a nonthermal excitation source to dissociate Si_2H_6 into photofragments that adsorb on the Si substrate and result in film growth.[1,2] By minimizing parallel reaction pathways with such a highly selective UV source, film morphology can be improved and semiconducting films with abrupt heterointerfaces and doping transitions can be deposited.[3] Such fabrication techniques will be crucial to the production of semiconductor material systems such as *n-i-p-i* doping superlattices and Si-$Si_{1-x}Ge_x$ strained-layer heterostructures for novel electro-optic and optoelectronic device applications.[4,5,6] Photoenhanced chemical vapor deposition (Photo-CVD) has been demonstrated by several methods including direct substrate illumination by deep ultra-violet (UV) lamp sources[7] and excimer lasers,[8] melt and recrystallization of amorphous layers by UV lasers,[9] and other techniques using UV radiation.[10,11] Photo-CVD of amorphous Si:H films has been studied in depth since, under photolytically sustained deposition conditions, the substrate temperature can be used to control the H content of deposited films, and can therefore control various properties of the films such as the index of refraction and the photoconductivity.[12,13,14] Using an ArF excimer laser as the Photo-CVD source presents distinct advantages over other Photo-CVD methods. A photon energy of $h\nu$ = 6.4 eV readily dissociates Si_2H_6 by single photon absorption,[14] producing Si-containing radicals that lead directly to film growth. Orienting the laser so that it passes parallel to the substrate surface allows reactive molecules to be created near the growth surface without an appreciable substrate temperature rise. In our study, epitaxial films were deposited at growth rates of 1-10Å/min, which is suitable for superlattice-type applications.

In this paper we present dependencies of growth rate and film morphology on process parameters and discuss the results in terms of a growth kinetic model. The results indicate that the dominant growth precursor has a sticking coefficient of ≥0.6, and that the sticking coefficient is insensitive to substrate temperature in the temperature regime of laser-controlled deposition (less than ~350° C). At laser intensity and Si_2H_6 partial pressure conditions such that initial photofragment concentrations are greater than $\sim 10^{13}$ molecules/cm^3, epitaxial growth is not achieved. Growth rates are somewhat decreased as the distance between the laser beam axis and the substrate is increased, but significant deposition still occurs for beam-to-substrate distances of ~2 cm, indicating that the dominant growth precursor is a resonably kinetically stable radical with respect to gas phase reactions.

2. EXPERIMENTAL

The substrate cleaning techniques and the ultra-high vacuum photo-CVD system used to deposit the films have been described previously.[1,2] Briefly, the Si substrates are solvent and RCA cleaned, and, immediately prior to loading into the ultra-high vacuum (UHV) deposition chamber, a HF dip is performed to H passivate the substrate surface.[15,16] The ArF excimer laser outputs 20 ns pulses at a maximum repetition rate of 80 Hz, and the pulse energy can be varied from 15 to 200 mJ/pulse. In order to deposit onto a larger area of the 10 cm diameter substrates, the initial 20 × 10 mm beam cross-sectional area is converted to 45 × 2 mm with beam

(Received January 13, 1992)

0361-5235/1992/1401-791$5.00©92 TMS

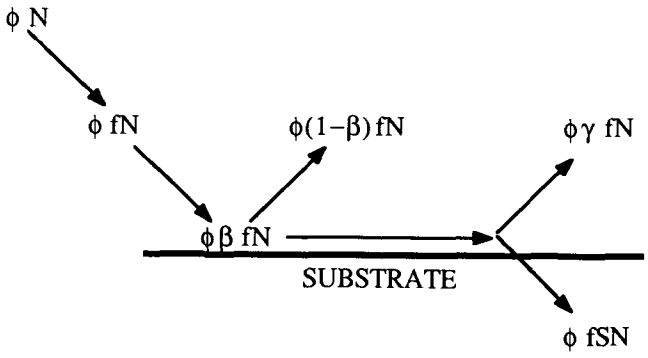

Fig. 1 — A schematic representation of the fraction of each photofragment that incorporates into the film. The quantum yield is ϕ, the number of excited disilane molecules is N, the fraction of the photoproduct which diffuses toward the substrate and survives gas phase reaction is represented by the factor f, and β is the fraction which is physisorbed on to the substrate surface. The fraction of Si lost through desorption from the surface is γ, and S is the total sticking probability of the photofragment.

shaping optics. The beam is passed tangentially under the substrate to avoid laser-induced damage or heating, and enters and exits the chamber through quartz windows which are purged with 1600 to 2400 sccm of He to prevent Si deposits from forming and absorbing the beam. Pure Si_2H_6 is mass-flow controlled at flow rates ranging from 14 to 114 sccm and is introduced through a 10 cm wide gas tee with eight equally spaced pinholes, which is positioned 9 cm from the edge of the substrate and 2 cm below it.

An oxide/polysilicon stack covers a third of the substrate surface so that the laser-deposited film thickness profile can be measured with a spectrophotometer. Silicon etching during the RCA clean was taken into account when determining the deposited film thickness.[17] During the RCA clean, the polysilicon film is etched 63 ± 4Å, as determined by measurements performed before and after cleaning and a HF dip. The average film thickness was divided by the deposition time to calculate the average growth rate over an area of ~90 cm^2 on the substrate surface. The number of Si atoms incorporated into the film was calculated from the average film thickness, the measured area, and the atomic number density of solid Si (5×10^{22} atom/cm^3). When the beam is within 1 mm of the substrate, peak growth rates are typically ~1.8 times the average growth rate.

3. MODEL

In order to estimate the fraction of photolysis products that can reach the film by diffusion from the beam-excited region to the substrate, the quantum yields for formation of the various photolysis products must be estimated and the gas phase kinetics of the individual products must be considered. The fraction of each photofragment that incorporates into the film is represented schematically in Fig. 1. The number of each photoproduct is given by the product of the quantum yield for the species, ϕ, and the number of excited Si_2H_6 (Si_2H_6*), N. The fraction of the photoproduct which diffuses toward the substrate and survives gas phase reaction is represented by the factor f. Of the photoproducts that strike the substrate surface a fraction β is physisorbed and a fraction (1-β) is reflected back into the bulk of the gas. Once physisorbed on to the substrate surface, the presursor can migrate along the substrate surface and Si can be removed from the surface if the precursor desorbs from the surface, or if the precursor reacts heterogeneously to form molecules which desorb from the surface (γ). Solid Si is deposited if the precursor chemisorbs (S) into the film.

The dissociative quantum yield in Si_2H_6 photolysis at 193 nm has been measured to be 0.7 ± 0.1, although the yield for loss of Si_2H_6 can increase to ~4 when the time between laser pulses is less than the gas residence time in the laser beam volume.[18] The additional 30% of the Si_2H_6* is thought to decay radiatively or be stabilized collisionally. The increased yield at high laser repetition rates is accompanied by broad infrared emissions and is presumably due to the onset of gas-phase nucleation initiated by secondary photolysis of long-lived photoproducts or a buildup of unsaturated silicon hydrides.[19] Gas phase nucleation effects can explain observations of amorphous Si:H powder formation at high laser repetition rates.[20] However, it is unlikely that significant gas phase nucleation is occurring when epitaxial films are produced in our reactor because it would interfere with epitaxial growth.

Denoting the deposition yield by α, the following expression can be written involving the quantum yields, ϕ, the fraction surviving diffusion to the substrate, f, and the total sticking probability, S, of each photofragment "i":

$$\alpha = \sum_i \frac{1}{2} a_i f_i S_i \phi_i, \tag{1}$$

where a_i is the number of Si atoms produced in the photolysis step that are contained in the photofragment of interest, and $\Sigma_i \phi_i = 0.7$.

The number of Si_2H_6 molecules directly under the substrate that absorb a photon can be estimated by using the photoabsorption cross-section of Si_2H_6 at 193 nm, $\sigma = (3.4 \pm 0.3) \times 10^{-18}$ cm^2,[18] the Si_2H_6 concentration, n, and the path length of the beam inside the chamber. The differential equation describing the change of laser beam intensity, $I(z)$, as a function of propagation distance, z, is

$$-dI(z) = \sigma n I(z)\, dz. \tag{2}$$

The Si_2H_6 concentration, n, ranges from 1.6×10^{14} to 1.3×10^{15} cm^{-3} for the Si_2H_6 partial pressures between 5 and 40 mTorr used in this work. With the chamber geometry shown in Fig. 2, Eq. 2 is in-

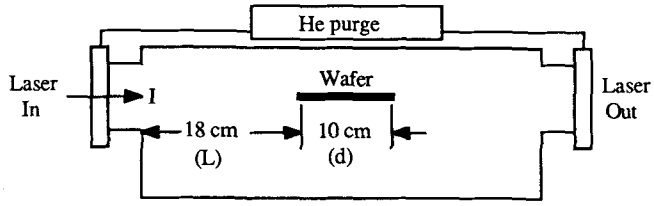

Fig. 2 — Schematic of the photo-chemical vapor deposition system showing relevant chamber dimensions.

tegrated to give the intensity absorbed by the Si_2H_6 molecules in the beam and under the substrate.

$$I_a = Ie^{-\sigma nL}(1 - e^{-\sigma nd}), \tag{3}$$

where L and d are as shown in Fig. 2, and I is the measured laser intensity in $J/cm^2 \cdot$ pulse that enters the chamber through the laser inlet window. The number of photons absorbed per pulse, N, is I_a divided by the photon energy, $h\nu$, and multiplied by the beam cross sectional area, WH. Thus,

$$N = \frac{I}{h\nu} WHe^{-\sigma nL}(1 - e^{-\sigma nd}), \tag{4}$$

where W is the beam width, and H is the beam height. Under optically thin absorption conditions, which occur for Si_2H_6 partial pressures of $\leq$35 mTorr, Eq. 4 reduces to

$$N = I\sigma nV/h\nu, \tag{5}$$

where V is the volume of the beam under the substrate, which will be referred to as the "active volume." The number, N, is also the number of excited Si_2H_6 molecules, Si_2H_6*, in the active volume.

The deposition yield can be measured by dividing the number of Si atoms incorporated into the film by $2N$. In terms of the average growth rate, $\langle G \rangle$, the expression for the deposition yield is given by Eq. 6,

$$\alpha = (\langle G \rangle A\rho)/(2N\Omega), \tag{6}$$

where A is the measured film area, ρ is the atomic number density of solid Si, and Ω is the laser repetition rate.

By combining the two expressions for α (Eqs. 1 and 6), a growth kinetic model can be constructed to give an expression for the average growth rate, $\langle G \rangle$,

$$\langle G \rangle = \frac{I\Omega\sigma nV}{A\rho h\nu} \sum_i a_i f_i S_i \phi_i, \tag{7}$$

where we have used Eq. 5 to write $\langle G \rangle$ as a function of the process parameters. This model describes the average growth rate expected for laser-controlled deposition. The exact form of Eq. 7 depends on the gas phase reaction of the dominant growth precursor through the factor f, and the temperature dependence of the average growth rate is expressed through the factor S. As described in the following section, the growth rate is not a strong function of the substrate temperature for temperatures below ~350° C. Thus, for low substrate temperatures, a simple expression involving the process parameters can be used to predict the average growth rate for films deposited using ArF excimer laser photolysis of Si_2H_6. Using Eq. 1, the average growth rate is simply,

$$\langle G \rangle = \frac{I\Omega\sigma nV}{A\rho h\nu} 2\alpha, \tag{8}$$

where α is the deposition yield, which can be determined by using Eq. 6 and measurements of the average growth rate.

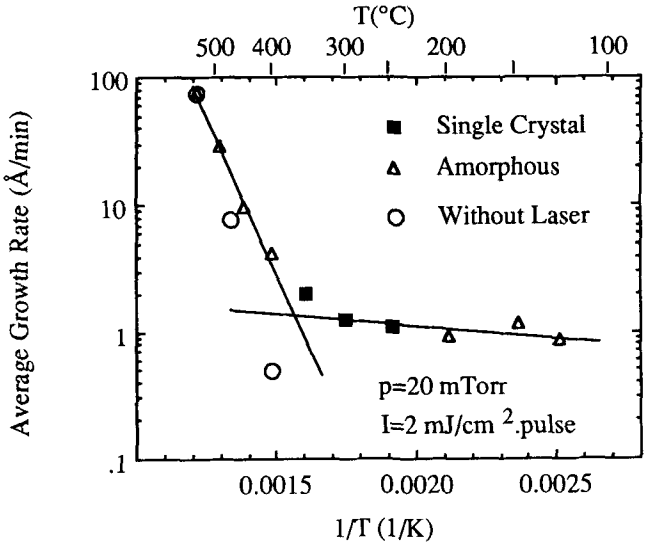

Fig. 3 — Average growth rate vs substrate temperature, T. The total pressure was 600 mTorr and the He flow rate was 1600 sccm.

4. EXPERIMENTAL RESULTS

The effects of substrate temperture, Si_2H_6 partial pressure, and laser intensity on the average growth rate have been characterized. From the results shown in Fig. 3, it is apparent that in the temperature regime where growth is laser-controlled, *i.e.* less than ~350° C, growth rates are not a strong function of substrate temperature. Above 350° C, growth rates are significantly increased due to pyrolytic decomposition of Si_2H_6. Included in Fig. 3 are three experiments performed without the laser, which verify that Si_2H_6 pyrolysis becomes appreciable above 350° C. Amorphous films are produced when pyrolytic growth begins to dominate, presumably due to insufficient adatom mobility and the loss of H passivation. At temperatures below 250° C, the breakup of Si_xH_y species on the Surface may be incomplete, leading once again to amorphous films.[13]

The expression in Eq. 8 indicates that the average growth rate should increase linearly with Si_2H_6

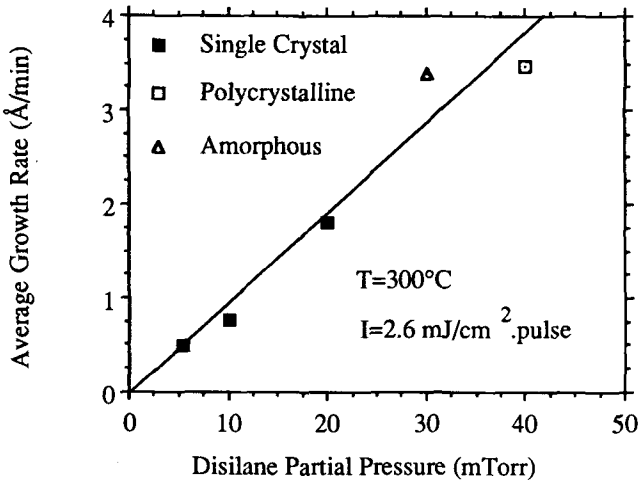

Fig. 4 — Average growth rate versus Si_2H_6 partial pressure, p. The total pressure was 600 mTorr and the He flow rate was 1600 sccm.

concentration and laser intensity, as observed in Figs. 4 and 5, respectively. As the Si_2H_6 partial pressure is increased above ~35 mTorr, the growth rate will begin to exhibit a sublinear dependence on Si_2H_6 concentration since optically thin absorption conditions will no longer be in effect and the number of Si_2H_6* molecules will be given by Eq. 4. The value of 35 mTorr is the point where the term $\exp(-\sigma nL)$ in Eq. 4 is reduced to ~0.9. A further increase in Si_2H_6 concentration results in significant absorption of the laser beam in the region between the laser inlet window and the substrate. At this point, the growth rate is no longer a linear function of the Si_2H_6 partial pressure. The fact that the growth rate increases linearly with increasing laser intensity and Si_2H_6 partial pressure indicates that the deposition yield depends directly on the generation of photolysis products. The results shown in Fig. 4 indicate that epitaxy is lost at Si_2H_6 partial pressures of 30 mTorr and laser intensities of 2.6 mJ/cm^2 · pulse, which is expected to produce a Si_2H_6* concentration

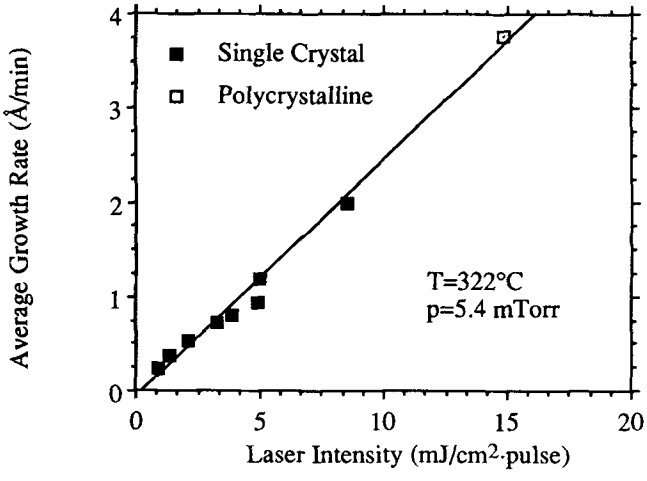

Fig. 5 — Average growth rate vs laser intensity, I. The total pressure was 600 mTorr and the He flow rate was 1600 sccm.

of $\sigma In/h\nu \sim 8 \times 10^{12}$ cm^{-3}. From the results shown in Fig. 5, polycrystalline films are deposited when the laser intensity is increased to 15 mJ/cm^2 · pulse. At a Si_2H_6 partial pressure of 5.4 mTorr used for these experiments, the concentration of Si_2H_6* is expected to be $\sim 9 \times 10^{12}$ cm^{-3}. It is clear that a transition from single crystal to polycrystalline growth occurs when the product of laser intensity and Si_2H_6 partial pressure results in photofragment concentrations of $\sim 10^{13}$ cm^{-3}. The effect could be due to excessive precursor fluxes or gas phase nucleation processes. As the deposition rate becomes comparable to the H_2 desorption rate, H desorption may not be rapid enough to allow Si_xH_y complexes to decompose into species which can form an epitaxial film.[13] A higher photofragment concentration may also increase the chance for homogeneous reaction between the photofragments, possibly leading to Si_xH_y particulates being formed in the gas phase. A significant flux of such particulates onto the growing film would induce polycrystalline or amorphous growth.

Using the data presented in Figs. 3–6 and Eq. 6, it is found that α, the yield for solid Si film formation, is 0.20 ± 0.04, where the uncertainty in this value is one standard deviation. In all of the experiments of Figs. 3–6, the top of the laser beam was within ~1 mm of the substrate surface. It is expected that moving the laser beam further from the substrate will result in lower deposition yields, and future experiments are planned to address this issue.

5. DISCUSSION

The photochemistry of Si_2H_6 is quite complex, and the predominant photoproducts of Si_2H_6 photolysis responsible for sustaining low temperature deposition are yet to be conclusively determined. It has been proposed that a major decomposition pathway is the formation of SiH_3SiH and H_2, although this has yet to be verified spectroscopically.[13] The 193 nm photons from an ArF excimer laser contain enough energy to break several combinations of Si-Si and Si-H bonds in Si_2H_6, and it is estimated that there are at least twenty energetically possible decomposition pathways for single photon Si_2H_6 photodissociation involving at least fourteen distinct photoproducts.[21] The only stable molecules produced are SiH_4 and H_2, while the bulk of the photoproducts are thought to be from two groups of silicon hydride species: monoradicals such as SiH_3, H_3SiSiH_2, and H_2SiSiH, and/or the closed-shell disilicon species, H_2SiSiH_2 and $Si(H_2)Si$.[18] These transient species are reasonably kinetically stable and react much slower with Si_2H_6 than do members of a third group containing the silylenes and silylidynes SiH_2, SiH_3SiH, SiH and $SiSiH_2$, which are believed to make up less than 20% of the photolysis products.[18] The molecules responsible for Si deposition are most likely produced from the initial pho-

tolysis steps shown in Table I. Other products which can be produced include SiH and atomic Si, but these are believed to arise mainly from multi-photon processes which are unlikely to be important for the low laser intensities used in our experiments.[22] The identification of SiH_4 and SiH_3 as primary photolysis products has been confirmed by using time-resolved infrared diode laser absorption spectroscopy and tunable diode laser flash kinetic spectroscopy, respectively, and the quantum yields for production of these molecules have been measured to be 0.1 ± 0.03 for SiH_4 and 0.05 ± 0.05 for SiH_3.[18,23] The radical SiH_2 is also formed in ArF laser Si_2H_6 photolysis.[24] Although the yield for this radical has yet to be measured directly, it may be ~0.1 since SiH_2 is formed in conjunction with SiH_4 in several of the Si_2H_6* decomposition pathways. The quantum yields for the remaining photolysis products are not known. Silylsilylene, SiH_3SiH, can form the stable, closed-shell isomer H_2SiSiH_2 by a 1,2 hydrogen shift.[25] The radical H_2SiSi can form the lower energy isomer, $Si(H_2)Si$, and the monoradical H_3SiSiH_2 is thought to be relatively stable.[24] Using fluorescence emission spectroscopy, researchers have consistently identified silylidyne radicals, SiH, as a photo-product of ArF excimer laser dissociation of Si_2H_6. The fluorescence intensity of SiH* scales as the square of laser intensity, indicating that its presence is likely due to a cascade photodissociation process where the primary photofragments SiH_3[22] and SiH_3SiH[13] absorb a photon during the same laser pulse. Evidence also exists for the creation of atomic Si by a three-step cascade absorption mechanism.[22] The SiH* concentration has been found to have little effect on film growth rates,[13] indicating that this species is produced in concentrations much lower than the species responsible for the bulk of the film growth. This is a reasonable assumption to make for our processing conditions where typical beam intensities excite only ~1% of the source gas in the beam. We therefore neglect multi-photon processes in this paper.

Next, the gas phase chemical reactions of the various photofragments are discussed. Because of the pulsed nature of the excitation, the time evolution of each photofragment concentration will approximately follow a differential equation of the form

$$-\frac{\partial n_i}{\partial t} = \frac{n_i}{\tau} + k_{io} n n_i + 2k_i n_i^2 + \sum_j k_{ij} n_j n_i \qquad (9)$$

where n_i is the photofragment concentration generated in the active volume, τ is the average time required to diffuse to the chamber walls, k_{io} is the rate constant for the removal of the photofragment by Si_2H_6, k_i is the rate constant for the recombination reaction between photofragments, and k_{ij} is the rate constant for the reaction of the photofragment with other photofragments of concentration n_j. It may be noted that Eq. 9 is only expected to give a first order estimate of the effects of diffusion on the photofragment concentration.

The average time, t, required for the photofragments to diffuse a distance x to the substrate is $x^2/2D$,[20] where D is the diffusion constant. If we neglect the time dependence of n_j on the right hand side of Eq. 9 and replace n_j with an average value, $\langle n_j \rangle$, the general solution to Eq. 9 is given by Eq. 10,

$$n_i(t) = \frac{C n_i(0) \exp(-tC)}{C + 2k_i n_i(0)[1 - \exp(-tC)]}, \qquad (10)$$

$$\text{where } C = k_{io} n + \sum_j k_{ij} \langle n_j \rangle + 1/\tau$$

The final form of Eq. 10 depends on the photofragment being considered, which determines what gas phase reaction mechanism dominates the loss process. When considering the SiH_2 radical concentration, it is expected that the dominant gas phase reaction is with Si_2H_6, which proceeds with an absolute rate constant of $k_{io} \cong 1.5 \times 10^{-10}$ cm^3/molecules·s in a He ambient at total pressures near 1 Torr.[26] In this case, Eq. 10 would reduce to $n_i(0)\exp(-tk_{io}n)$. The SiH_3 concentration is likely to be influenced most by the recombination reaction, which proceeds with a rate constant of $k_i \sim 10^{-10}$ cm^3/molecule·s,[23,27] and

Table I. The Quantum Yields, ϕ, the Fractions of Photoproducts Surviving Diffusion, f, and the Sticking Coefficients, S, for Various Dissociation Steps in 193 nm Si_2H_6 photolysis. Values of f are Estimated Using Eq. 11 for a Si_2H_6 Partial Pressure of 10 mTorr and Diffusion Times 40 μs and 3 ms. References used for the values of ϕ and S are Given in Brackets Next to Each Value.[1] Assumed Values for ϕ.[2] Estimated Values for S Based on a Deposition Yield of 0.2.

Dissociation Step	ϕ	Molecule	$f(t = 40\ \mu s)$	$f(t = 3\ ms)$	S
$Si_2H_6 + h\nu \rightarrow SiH_2 + SiH_4$	0.1 [18]	SiH_2	0.07	0.00	0.7 [30]
$Si_2H_6 + h\nu \rightarrow SiH_3SiH + H_2$	0.4[1]	H_2SiSiH_2	0.50	0.40	≥0.6[2]
$Si_2H_6 + h\nu \rightarrow 2SiH_3$	0.05 [23]	SiH_3	0.50	0.46	0.1 [29]
$Si_2H_6 + h\nu \rightarrow H_2SiSi + 2H_2$	0.1[1]	H_2SiSi	0.48	0.03	≥0.6[2]
$Si_2H_6 + h\nu \rightarrow H_3SiSiH_2 + H$	0.05[1]	H_3SiSiH_2	0.50	0.46	0.1 [29]

the $2k_i n_i(0)$ term in Eq. 10 would dominate the expression for the SiH_3 concentration. For H_2SiSiH_2, the removal of this species in the gas phase is slow and may depend on *both* the laser beam intensity and the Si_2H_6 partial pressure.[24] Therefore, it appears that the dominant gas phase reaction is with photolysis products. The radical H_2SiSi is expected to react with Si_2H_6 because it is a silylene,[18] and H_3SiSiH_2 is expected to behave similarly to SiH_3 since both of these are monoradicals.

The fraction of each photofragment, "*i*", which survives reaction as it diffuses to the substrate can therefore be estimated by

$$f_i = (1/2)[n_i(t)/n_i(0)], \quad (11)$$

where the factor of one-half indicates that only half of the photofragments are expected to diffuse toward the substrate. A more rigorous estimate of f_i would require the diffusion equation to be solved with the appropriate boundary conditions. The estimated values of f_i for the various growth precursors and their total sticking probabilities are listed in Table I. It is apparent from the values of $\phi(SiH_2)$ and $f(SiH_2)$ that the SiH_2 radical contributes little solid Si to the films. Also, the values of $\phi(SiH_3)$ and $S(SiH_3)$ indicate that the radical SiH_3 is not the dominant growth precursor. Silane, SiH_4, does not form solid films at the substrate temperatures used in this work, and hence can be ruled out as a possible growth precursor. Little is known about the role of H_2SiSiH_2, H_2SiSi, or H_3SiSiH_2 in CVD conditions used in our work. In calculating the values of $f(H_2SiSiH_2)$, it is assumed that the dominant gas phase loss mechanism for H_2SiSiH_2 is recombination and that the reaction proceeds with a rate constant of $\sim 3 \times 10^{-11}$ cm^3/molecule·s. For the values of $f(H_2SiSi)$, it is assumed that H_2SiSi reacts with Si_2H_6 with a rate constant of $\sim 3 \times 10^{-12}$ cm^3/molecule·s. If H_2SiSi were to react gas kinetically with Si_2H_6 to form stable products such as Si_3H_8 and Si, it would be expected that little Si deposition would result from Si_2H_6 dissociation into H_2SiSi. However, H_2SiSi could react with Si_2H_6 to form H_2SiSiH_2 and H_3SiSiH, and these radicals could result in Si deposition. The gas phase kinetics of H_2SiSi are further complicated by the fact that this species can form the lower energy, bridged isomer, $Si(H_2)Si$. The amount of H_2SiSi that reacts with Si_2H_6 may therefore depend on how much of the H_2SiSi forms $Si(H_2)Si$ before reacting with Si_2H_6. The molecule H_2SiSiH_2 is a good candidate for being a dominant growth precursor since it is believed to be kinetically stable and can potentially be formed with high yield from Si_2H_6* photolysis. Additionally, H_2SiSiH_2 could easily contribute solid Si to the film if it decomposes into SiH_2 on, or very near, the substrate surface. Alternatively, if the π bond of this precursor is sufficiently weak to be reactive with the Si surface, it seems plausible that it could insert into the lattice in a manner similar to the insertion of SiH_2,[28] but requiring two H_2 desorption events instead of one. It is expected that the radical H_2SiSi has a large sticking coefficient since it is classified as a silylene and should behave similarly to SiH_2. The monoradical H_3SiSiH_2 should have a low surface loss probability similar to the monoradical SiH_3,[29] but if thermally dissociated into SiH_3 and SiH_2 on the surface, could lead to Si deposition. The assumed low surface loss probability, however, would preclude the possibility of H_3SiSiH_2 being the dominant growth precursor. Using the known quantum yields of $\phi(SiH_2) \sim 0.1$ and $\phi(SiH_3) \sim 0.05$ leaves ~ 0.55 of the Si_2H_6* molecules to dissociate into other species. If we assume that the bulk of the deposited Si is transported to the film by H_2SiSiH_2 and H_2SiSi, then the sticking coefficient that we assign to these precursors must be ≥ 0.6 in order to account for the measured deposition yield of 0.20 ± 0.04.

6. CONCLUSION

Homoepitaxial Si films can be controllably deposited at temperatures from 250–350° C if laser intensity and Si_2H_6 partial pressure conditions are such that the initial photofragment concentration is less than $\sim 10^{13}$ cm^{-3}. Growth rates vary linearly with laser intensity and Si_2H_6 partial pressure over a range of 1–15 mJ/cm^2·pulse and 5–40 mTorr, respectively, indicating that the deposition yield depends directly on the generation of photolysis products. At temperatures greater than ~400° C, deposition rates are increased due to Si_2H_6 pyrolysis. The deposition yield of Si atoms from ArF excimer laser photolysis of Si_2H_6 has been measured to be 0.20 ± 0.04, indicating that in order for film growth to result solely from the primary products in 193 nm Si_2H_6 photolysis, a sticking coefficient ≥ 0.6 must be assigned to the dominant growth precursor. A growth kinetic model has been developed based on the most likely dominant growth precursors responsible for Si deposition under laser-controlled growth conditions. The precursors responsible for the bulk of the deposited Si must be relatively stable with respect to gas phase reactions and are most likely H_2SiSiH_2, $Si(H_2)Si$, and possibly some small fraction of H_3SiSiH_2.

This work was sponsored by the NSF Presidential Young Investigator Program and the Science and Technology Center Program of NSF at the University of Texas at Austin, grant CHE-8920120.

REFERENCES

1. S. Lian, B. Fowler, D. Bullock and S. Banerjee, Appl. Phys. Lett. *58*, 514 (1991).
2. S. Lian, B. Fowler, S. Krishnan, L. Jung and S. Banerjee, Mat. Sci. Eng. *B 10* (3), 181 (1991).
3. D. Eres, D. Lowndes, D. Geohegan and D. Mashburn, Mater. Res. Soc. Symp. Proc. *101*, 355 (1988).
4. R. People, IEEE J. Quant. Elect. *QE-22*, *1696* (1986).
5. M. Gell, Phys. Rev. *B 38*, 7535 (1988).
6. G. Dohler, IEEE J. Quant. Elect. *QE-22*, 1682 (1986).
7. T. Yamazaki, H. Minakata and T. Ito, J. Electrochem. Soc. *137*, 1981 (1990).
8. Y. Suda, D. Lubben, T. Motooka and J. Greene, J. Vac. Sci. Technol. *B 7*, 1171 (1989).

9. S. Lombardo, P. Smith, M. Uttormark, D. Brunco, K. Kramer and M. Thompson, Appl. Phys. Lett. *58,* 1768 (1991).
10. J. Takahashi, Y. Utsumi, H. Akazawa, I. Kawashima and T. Urisu, Appl. Phys. Lett. *58,* 2776 (1991).
11. W. Milne, F. Clough, S. Deane, S. Baker and P. Robertson, Appl. Surf. Sci. *43,* 277 (1989).
12. Y. Mishima, M. Hirose, Y. Osaka, K. Nagamine, Y. Ashida, N. Kitagawa and K. Isogaya, Jpn. J. Appl. Phys. *22,* L46 (1983).
13. D. Eres, D. Geohegan, D. Lowndes and D. Mashburn, Appl. Surf. Sci. *36,* 70 (1989).
14. Y. Toyoshima, K. Kumata, U. Itoh and A. Matsuda, Appl. Phys. Lett. *51,* 1925 (1987).
15. B. Meyerson, F. Himpsel and K. Uram, Appl. Phys. Lett. *57,* 1034 (1990).
16. B. Anthony, L. Breaux, T. Hsu, S. Banerjee and A. Tasch, J. Vac. Sci. Technol. *B 7,* 621 (1989).
17. T. Niino and T. Tatsumi, Jpn. J. Appl. Phys. Lett. *29,* L1702 (1990).
18. J. Chu, M. Begemann, J. McKillop and J. Jasinski, Chem. Phys. Lett. *155,* 576 (1989).
19. J. Jasinski, J. Chu and M. Begemann, Mat. Res. Soc. Symp. Proc. *131,* 487 (1989).
20. T. Dietrich, S. Chiussi, H. Stafast and F. Comes, Appl. Phys. *A48,* 405 (1989).
21. H. Stafast, Appl. Phys. *A45,* 93 (1988).
22. Y. Muranaka, T. Motooka, D. Lubben and J. Green, J. Appl. Phys. *66,* 910 (1989).
23. S. Loh and J. Jasinski, J. Chem. Phys. *95,* 4914 (1991).
24. J. Jasinski, Chem. Phys. Lett. *183,* 558 (1991).
25. R. Becerra and R. Walsh, J. Phys. Chem. *91,* 5765 (1987).
26. J. Jasinski and J. Chu, J. Chem. Phys. *88,* 1678 (1988).
27. N. Itabashi, K. Kato, N. Nishiwaki, T. Goto, C. Yamada and E. Hirota, Jpn. J. Appl. Phys. *28,* L325 (1989).
28. D. Metzger, K. Hesch and P. Hess, Appl. Phys. *A 45,* 345 (1988).
29. Y. Matsui, A. Yuuki, N. Morita and K. Tachibana, Jpn. J. Appl. Phys. *26,* 1575 (1987).
30. T. Fuyuki, B. Allain and J. Perrin, J. Appl. Phys. *68,* 3322 (1990).